

# Molecular Orbital Calculations for the Formation of GaN Layers on Ultra-thin AlN/6H-SiC Surface Using Alternating Pulsative Supply of Gaseous Trimethyl Gallium (TMG) and NH<sub>3</sub>

Seeyearl Seong\* and Jin-Soo Hwang†

Computer Aided Molecular Design Center at Soong-Sil University, Dongjak-Ku, Sangdo 5-Dong 1-1, Seoul 156-035, Korea

†Korea Research Institute of Chemical Technology, Yusong-Ku, Jang-Dong 100, P.O. Box 107, Taejon 305-343, Korea

Received July 18, 2000

The steps for the generation of very thin GaN films on ultrathin AlN/6H-SiC surface by alternating a pulsative supply (APS) of trimethyl gallium and NH<sub>3</sub> gases have been examined by ASED-MO calculations. We postulate that the gallium cluster was formed with the evaporation of CH<sub>4</sub> gases *via* the decomposition of trimethyl gallium (TMG), dimethyl gallium (DMG), and monomethyl gallium (MMG). During the injection of NH<sub>3</sub> gas into the reactor, the atomic hydrogens were produced from the thermal decomposition of NH<sub>3</sub> molecule. These hydrogen gases activated the Ga-C bond cleavage. An energetically stable GaN nucleation site was formed *via* nitrogen incorporation into the layer of gallium cluster. The nitrogen atoms produced from the thermal degradation of NH<sub>3</sub> were expected to incorporate into the edge of the gallium cluster since the galliums bind weakly to each other (0.19 eV). The structure was stabilized by 2.08 eV, as an adsorbed N atom incorporated into a tetrahedral site of the Ga cluster. This suggests that the adhesion of the initial layer can be reinforced by the incorporation of nitrogen atom through the formation of large grain boundary GaN crystals at the early stage of GaN film growth.

**Keywords :** GaN, CVD, MO-Theory.

## Introduction

The device quality of epitaxially grown gallium nitride films with low defect densities and dopant concentrations is blocked by the lattice mismatch between epi-films and substrates. Crystal quality, surface morphology, electrical and optical properties of the films depend in a critical way on the thickness and quality of buffer layers employed to overcome lattice mismatch.<sup>1</sup> The initial monolayer of a heteroatomic interface plays an important role in determining the growth habits of subsequent layers. Nucleation is an initial stage of any phase transformation, including crystallization.<sup>1,2</sup> During its growth, GaN quality is entangled severely by the gas phase interactions between trimethyl gallium (TMG) and ammonia, the commonly used growth precursors. A review of precursors for preparation of group III-nitrides was published recently.<sup>3</sup> One of the popular precursors for the synthesis of GaN epi-films is TMG and ammonia. The gas phase structure and decomposition mechanism of TMG have been studied by Buchan.<sup>4,5</sup> In ambient H<sub>2</sub>, a chain reaction takes place giving methane, methyl radical, and monomethyl gallium. Bock *et al.* investigated the strength of gallium carbon bonds in TMG, DMG, and MMG.<sup>6</sup> Further decomposition of MMG into CH<sub>3</sub> and gallium is not a dominant gas-phase reaction according to Tirto-widjojo and Pollard.<sup>7</sup> Chong *et al.* studied the thermal decomposition of trimethylgallium and trimethylgallium-ammonia adduct (TMG : NH<sub>3</sub>), using Fourier Transform infrared spectroscopy. The activation energy for TMG : NH<sub>3</sub> decomposition was determined to be 63 kcal/mol.

The CH<sub>3</sub> group is generated as the intermediate species during the adduct decomposition under the experimental range

of pressure. Chen *et al.*<sup>8</sup> studied the thermal decomposition of TMG using molecular beam sampling mass spectroscopy. They found that TMG decomposes by successively releasing its three methyl radicals. The activation energy for the rupture of the Ga-C bonds is between 52.6-64.6 kcal/mol. The reaction of trimethyl gallium and ammonia on silicon wafer has been analyzed by Conner *et al.* using FT-IR.<sup>9</sup>

*In situ* IR laser diode spectroscopy<sup>10</sup> has been documented for the decomposition of TMG above a reactive surface. Marsel *et al.* showed that the decomposition of TMG is an intramolecular process.<sup>11</sup> Theoretical studies using *ab-initio* molecular orbital calculations have been carried out for the Cl removal reaction induced by H<sub>2</sub> in chloride atomic layer epitaxy of GaAs growth,<sup>12</sup> however, theoretical studies on GaN growth are few. The mechanism for Ga-N bond formation on  $\alpha$ -Al<sub>2</sub>O<sub>3</sub> surface in HCl/He/NH<sub>3</sub>/Ga system (HVPE method) has been studied using the semi-empirical ASED-MO (Atomic Superposition and Electron Delocalization-Molecular Orbital) method.<sup>13</sup> Recently, GaN growth in MBE-like conditions has been studied by Monte-Carlo simulation.<sup>14</sup> The quality of the growth front can be improved by using a small Ga flux for a fixed temperature and V/III ratio or by reducing the V/III ratio at a given temperature. The study of the nucleation mechanism is very important, as the initial monolayer determines the growth habits of subsequent layers. We have investigated Ga-N bonding, which affect growing patterns, size of the grain boundary and optical properties.

## Theoretical Model

The AlN buffer is widely used for GaN growth because of

its stability at high temperature and close lattice parameters to GaN crystal.<sup>15</sup> Due to computation limits, cluster models are usually taken for the study of bulk systems.<sup>16</sup> For the analysis of bonding, a two-layer [0001]-AlN cluster,  $[Al_{37}N_{37}]$ , has been taken. The  $Al_{37}N_{37}$  cluster represents the wurzite type c-face of AlN buffer. For the study of Ga-N bond formation in the metal organic chemical vapor deposition (MOCVD) process using TMG and  $NH_3$  as a reactants, we have conducted an ASED-MO for the reaction on AlN buffer layer. The anions and cations in AlN are tetrahedrally coordinated. The structure is wurzite, with lattice constants  $a = 3.11\text{Å}$ ,  $c = 4.98\text{Å}$  and  $c/a = 1.60\text{Å}$ .<sup>17</sup> The employed  $Al_{37}N_{37}$  cluster model is shown in Figure 1. Both Al and N ions are present, making this a suitable model for homolytic dissociative chemisorption studies.

The cluster contains 32 three-fold and 18 two-fold, 24 four-fold coordinated cations and anions. The nitrated AlN surface model is constructed by putting nitrogen atoms on the surface  $Al^{3+}$  atoms. The  $NH_3$  molecule dissociatively adsorbs on the GaN surface.<sup>18</sup> Hydrogen atoms on the surface are mobile and easily desorb in a recombinative fashion. Thus, the nitrated Al-N surface is considered to be covered with nitrogen atoms. Accordingly, the model for the nitrated surface should have  $[Al_{37}N_{56}]^{-57}$  formula since it has extra nitrogen atoms (Figure 1b). Gallium atoms are repulsive to one fold site of  $[Al_{37}N_{56}]^{-57}$  cluster, however, they strongly adsorb on three-fold sites of nitrogen layer (Figure 1a). There are two different types of three-fold sites. Gallium adsorption on "a" site will give a wurzite structure, whereas adsorption on "b" site gives a cubic structure. Nonetheless, the differences in growth mechanisms between the two structures are not known.

**Calculation Method.** ASED-MO<sup>19</sup> is a semi-empirical theoretical approach that based on the distribution of electronic charge density into the free atomic part and an electron delocalization for the bond formation component. As the atoms approach each other to form a molecule, the forces on the nuclei are integrated into a repulsive energy of rigid atomic densities and an attractive energy resulting from electron delocalization.

In the ASED-MO method, the energy of atomic superposition is obtained from real atomic densities and the energy of electron delocalization energy is estimated by the modified extended Huckel method. This technique has been used in studies involving CH bond activation on  $[1010]AlN$ <sup>16</sup> and metal surfaces.<sup>19</sup> The atomic parameters used for Al, N, C,

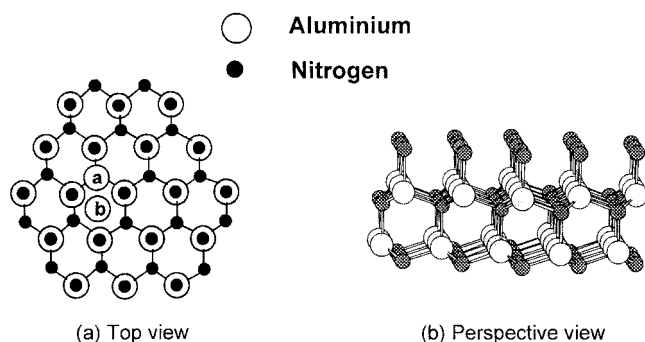


Figure 1. Crystal structure of wurzite type AlN clusters.

and H in all calculations in this paper are listed in Table 1.

The calculated bond length of diatomic molecule AlN was 1.79 Å. The ionization potentials of N are decreased 2 eV from the atomic values to adjust the ionicity of bulk structure.<sup>22</sup> The structural parameters in the present study are optimized within an error range of 0.01 Å in bond length and 3 degree in bond angles.

The cluster band structure, shown in Figure 2 can be labeled in three parts. The lower bands under the fermi level are filled Al-N bonding orbitals. Their characters are predominantly N2s and N2p. The empty antibonding counterparts are localized primarily on Al and divide into bulk and surface bands. The bulk Al bands lie in the high energy level above 1.7 eV. The calculated band gap between the surface band and empty LUMO of  $[Al_{37}N_{37}]$  cluster model is 7.0 eV, fairly close to

Table 1. Atomic orbital parameters used in the calculation: Principal quantum number n, Slater exponent (au), ionization potential IP (eV).

Atom	Orbital	Slater Exponent (a.u.)	Ionization Potential (eV)
Al <sup>a</sup>	3s	1.5213	-12.620
	3p	1.5041	-7.986
N <sup>b</sup>	2s	1.4737	-18.330
	2p	1.4670	-12.530
Ga <sup>c</sup>	4s	1.7667	-13.000
	4p	1.5554	-8.000
C <sup>d</sup>	2s	1.6580	-14.590
	2p	1.6180	-9.260
H <sup>d</sup>	1s	1.2000	-13.600

<sup>a</sup>Reference 20. <sup>b</sup>Reference 21. <sup>c</sup>Reference 22. <sup>d</sup>Reference 23.

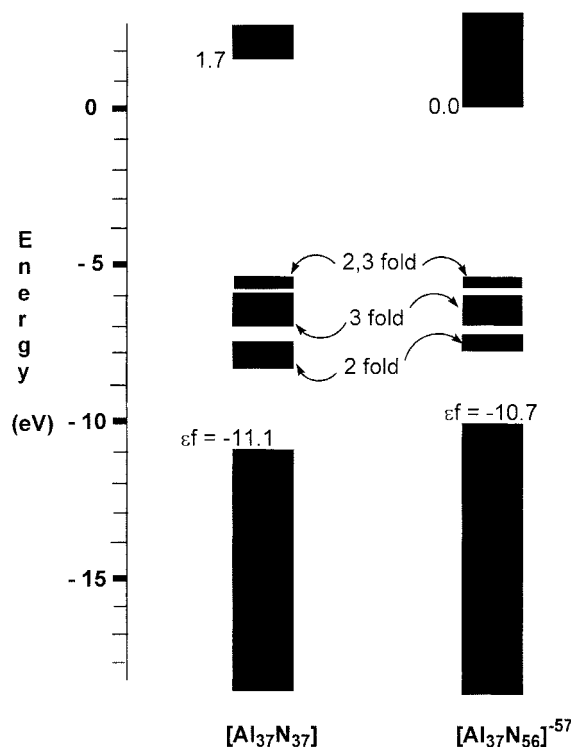


Figure 2. Electronic structure of  $[Al_{37}N_{37}]$  cluster and nitrated model  $[Al_{37}N_{56}]^{-57}$  cluster.

the optical band gap of 6.3 eV.<sup>24</sup>

The surface bands, which consist of surface Al atomic orbitals, lie between HOMO and LUMO, since they are more stable owing to the lower coordination numbers. The two-fold coordinated Al<sup>3+</sup> surface states are located at 2.8 eV above the N2p bands, whereas three-fold Al<sup>3+</sup> are at 4.1 eV. The bands at -5.7 eV represent mixed states of two- and three-fold sites. Thus, the two-fold Al<sup>3+</sup> site might be more active than the three-fold Al<sup>3+</sup> site on the extended surfaces. For the nitridated surface, the fermi level is pushed up to -10.7 eV due to the electron-rich N<sup>3-</sup> layer and a two-fold Al<sup>3+</sup> pushed up to -7.3 eV. The band gap between three-fold Al<sup>3+</sup> and N2p is 4.6 eV. Calculations by Anderson *et al.* show that the width and position

**Table 2.** Decomposition energies of TMG, DMG, and MMG (kcal/mol)

Reaction	<sup>a</sup> HF/SCF	ASED-MO	<sup>b</sup> Experimental
TMG → DMG + CH <sub>3</sub>	76.9	96.4	59.5
DMG → MMG + CH <sub>3</sub>	35.5	41.7	35.4
MMG → CH <sub>3</sub> + Ga	59.1	71.7	77.5

<sup>a</sup>Reference 6(a), (b). <sup>b</sup>Reference 6(c), (d).

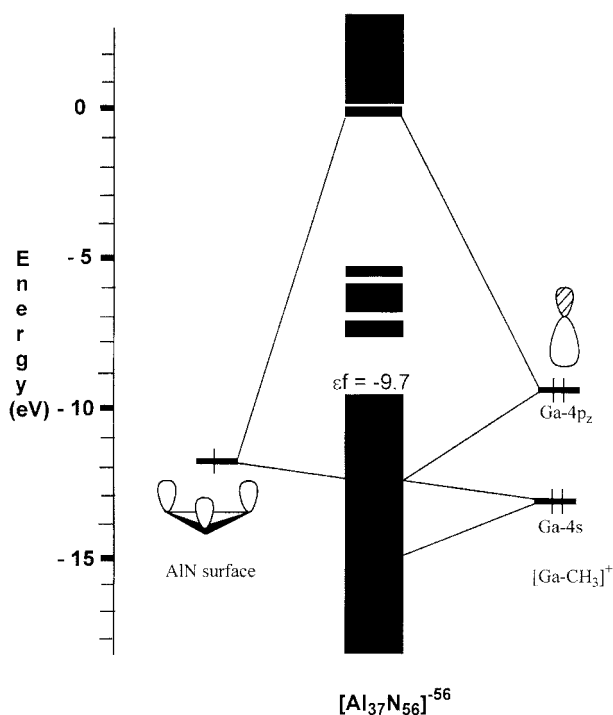


**Figure 3.** Orbital interactions between Ga-CH<sub>3</sub> molecule and nitridated AlN layer with one hole at nitrogen band.

of the filled N<sup>3-</sup> bands qualitatively agree with photoemission spectroscopic studies<sup>25,26</sup> and theoretical calculations.<sup>26,27</sup>

**Adsorptions of TMG and NH<sub>3</sub> on the AlN surface.** As studied earlier,<sup>28</sup> TMG is easily decomposed into its atomic components at high temperature. The  $\Delta E$  values for the decomposition of TMG, DMG, and MMG are compared in Table 2. ASED-MO calculations show the same trend as that obtained by *ab-initio* calculations. The Ga-C bond energy of MMG is quite close to the experimental result. We have analyzed the adsorption of the simple MMG molecule on the AlN surface using a MO diagram, for calculation convenience. The interactions of the MMG and N<sup>3-</sup> three-fold site is a closed shell repulsion (calculated binding energy, B.E. = -0.59 eV). Thus, the defect free surface is expected to be inactive. We postulate the nitridated surface with one electron deficient hole at N-2p band.<sup>16</sup> The calculated binding energy of MMG was 0.31 eV, whereas MMG binding on the surface with 2 holes was 4.21 eV. A correlation diagram of GaCH<sub>3</sub> adsorption on the N<sup>3-</sup> surface with one hole is shown in Figure 3. The s and p<sub>z</sub> hybridized lone pair orbital of gallium donates an electron to the hole in the nitrogen layer. Meantime, atomic Ga was repulsive toward the N<sup>3-</sup> surface; however, Ga<sup>+</sup>(2.71 eV), Ga<sup>2+</sup>(3.05 eV), Ga<sup>3+</sup>(4.73 eV) were strongly bound to the surface. Thus, Ga-CH<sub>3</sub> is believed to be dissociated on the nitridated AlN surface to yield Ga<sup>+</sup> and CH<sub>3</sub><sup>-</sup> anion. CH<sub>3</sub><sup>-</sup> is reported to bind to the Al<sup>3+</sup> site or desorbing quickly *via* recombinative with H<sup>+</sup> atoms.<sup>18</sup> The dissociative adsorption of GaCH<sub>3</sub> was energetically more favourable by 8.9 eV.

$$\Delta E_{stab} = (E_{Ga+ads} + E_{CH_3^-ads}) - E_{MMGads} \quad (1)$$

**Ga-N bond formation.** High quality GaN films of low defect density have been prepared by alternating a pulsative supply (APS) of trimethyl gallium and NH<sub>3</sub> gases. Nitrogen atoms were assumed to incorporate into the gallium formed by APS process.<sup>28</sup> We have postulated the steps for the generation of nucleation centers in the APS process as depicted in Figure 4. Firstly, the treatment of TMG-AlN surface with H<sub>2</sub> gas yields a gallium cluster by thermal decomposition of TMG.<sup>29</sup> A gallium cluster is expected to be formed with the evaporation of CH<sub>4</sub> gas as discussed earlier. Next, during NH<sub>3</sub> gas supply, the atomic hydrogens produced from the thermal decomposition of NH<sub>3</sub> also activate the Ga-CH<sub>3</sub> bond cleavage.<sup>30</sup> We found a gallium atom binds to the AlN surface with an energy of 4.73 eV by ASED-MO calculations.<sup>31</sup> The binding energy of Ga-NH<sub>2</sub> (monoammine gallium: MAG), a fragment of the TMG-NH<sub>3</sub> to the nitridated AlN surface, was 1.61 eV. This implies that atomic gallium adsorbs on the nitridated layer more strongly and has better wetting effect than Ga-

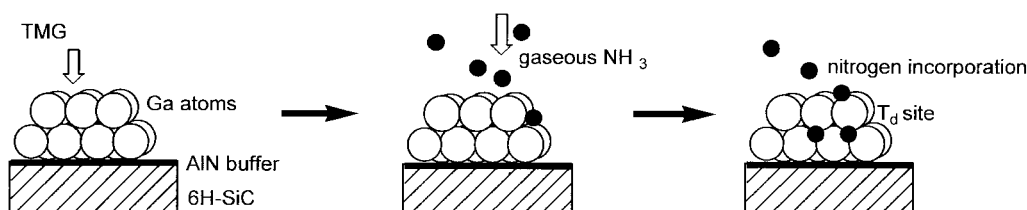


**Figure 4.** Postulated steps for the formation of GaN layers on AlN surfaces.

**Table 3.** Comparisons of GaN epi-films prepared by conventional MOCVD and APS pretreatment on AlN/6H-SiC<sup>28</sup>

Morphology /Physical Properties	Conventional MOCVD	APS pretreatment
double crystal x-ray diffractometer (FWHM)	260	143
defect density (ea/cm <sup>2</sup> )	$1.4 \times 10^8$	$2 \times 10^7$
relative PL intensity of I <sup>2</sup>	1	10
relative PL intensity of D-A (doner-acceptor)	1	1/10
net carrier concentration	$10^{16}$	less than $10^{16}$

NH<sub>2</sub>. Finally, an energetically stable GaN nucleation site is formed *via* nitrogen incorporation into the layer of gallium cluster. Nitrogen incorporation into the growing film is temperature dependant.<sup>9</sup> The nitrogen atoms produced from the thermal degradation of NH<sub>3</sub> incorporate into the edge of gallium cluster, where the gallium atoms bind weakly to each other.<sup>28</sup> The calculated Ga-Ga binding energy (0.19 eV) was quite close to the value obtained by Wang *et al.* (0.22 eV).<sup>32</sup> The structure was stabilized by 2.08 eV as adsorbed nitrogen atom incorporates into a tetrahedral site of a Ga cluster. This suggests that the adhesion of initial layer can be reinforced by incorporation of nitrogen atom.

It is known<sup>1</sup> if the free energy for substrate-medium adhesion ( $\alpha_s$ ) is weaker than the free energy for adhesion of crystal-medium interface ( $2\alpha$ ), a three dimensional crystal growth is favored, whereas a two dimensional growth is preferred for the opposite conditions ( $2\alpha < \alpha_s$ ). The crystals can be strongly adsorbed on the substrates and form a large grain if the changes in surface free energies are small ( $\Delta\alpha = 2\alpha - \alpha_s$ ).<sup>1</sup> The free-energy change ( $\Delta\alpha = 2\alpha_{\text{Ga-Ga}} - \alpha_{\text{Ga-N}}$ ) for the APS process will have a negative number because of weak Ga-Ga adhesion energy compare with Ga-N binding on AlN/6H-SiC surface. On the other hand, in the MOCVD procedure,  $\alpha$  and  $\alpha_s$  will be similar since both are determined by Ga-N bonding<sup>33,34</sup> energy and  $\Delta\alpha$  will be larger than that obtained from the APS process. Therefore, GaN buffer layers prepared by the APS process will have two-dimensional character (larger grain boundary) as well as fewer defects *via* formation of large size of nucleation site. All of these results agree well with those of experimental observations.<sup>28</sup>

### Conclusions

Both theoretical and experimental evidence support dissociative adsorption of TMG molecules on the AlN surfaces. The calculated dissociation energies of TMG derivatives were quite close to those of the experimental results. Gallium atoms are repulsive to the electron rich nitrogen surface; however, the positively charged galliums adsorb strongly. The Ga-CH<sub>3</sub> is expected to be dissociated into Ga<sub>(ads)</sub><sup>+</sup> and CH<sub>3</sub><sup>-</sup> anions, with a gain of stability by 8.9 eV. The nitrogen atoms formed *via* degradation of NH<sub>3</sub> gas incorporate into the tetrahedral site of the Ga cluster. The gallium clusters formed for the first step of APS treatment weakly bind to each other; however,

the clusters were stabilized by nitrogen incorporation. Experimentally, very thin GaN layers formed by the APS process improved the quality of films of low defect density ( $10^7$  cm<sup>-2</sup>). Therefore, APS pretreatment should promote the formation of large grains of GaN as well as fortify adhesion in the nucleation stage. The barrier of nitrogen incorporation into the gallium cluster was calculated to be low (0.19 eV). The ASED method yielded decent values for the dissociation of MMG and DMG compare with experimental results.

**Acknowledgment.** S. Seong thanks Professor A.B. Anderson of the Chemistry Department of Case Western Reserve University in U.S.A. for his helpful advice.

### References

- Givargizof, E. I. *Oriented Crystallization on Amorphous Substrates*; Plenum Press: New-York and London, 1991.
- Chernov, A. A. *Modern Crystallography III-Crystal Growth*; Springer-Verlag, New York, 1984.
- Neumayer, D. A.; Ekerdt, J. G. *Chem. Mater.* **1996**, *8*, 9.
- Larson, C. A.; Buchan, N. I.; Li, S. H.; Stringfellow, G. B. *J. Cryst. Growth* **1990**, *102*, 103.
- Jacko, M. G.; Price, S. J. *Can. J. Chem.* **1963**, *41*, 1560.
- (a) Bock, C. W.; Trachtman, M. *J. Phys. Chem.* **1994**, *98*, 95. (b) Nakano, T.; Hirano, T. *J. Appl. Phys.* **1995**, *78*, 251. (c) Jaco, M. G.; Price, S. J. *Can. J. Chem.* **1963**, *41*, 1560. (d) Oikawa, S.; Tsuda, M.; Morishita, M.; Mashita, M.; Kuniya, Y. *J. Cryst. Growth* **1988**, *91*, 471.
- Tirtowidjojo, M.; Pollard, R. *J. Cryst. Growth* **1988**, *93*, 108.
- Chen, Q.; Dapkus, P. D. *J. Electrochem. Soc.* **1991**, *138*, 2821.
- Mazzarese, D.; Tripathi, A.; Conner, W. C.; Jones, K. A.; Calderon, L.; Eckart, D. W. *J. Electronic. Mater.* **1989**, *18*, 369.
- Butler, J. E.; Bottka, N.; Sillmon, R. S.; Gaskill, D. K. *J. Cryst. Growth* **1986**, *77*, 163.
- Lee, F.; Gow, T. R.; Masel, R. I. *J. Electrochem. Soc.* **1989**, *136*, 2640.
- (a) Mochizuki, Y.; Takada, T.; Usui, A. *Jpn. J. Appl. Phys.* **1993**, *32*, L197. (b) Mochizuki, Y.; Takada, T.; Sakuma, T.; Handa, S.; Sasaoka, C.; Usui, A. *J. Cryst. Growth* **1994**, *135*, 259.
- Manuscript submitted for publication.
- Wang, K.; Singh, J.; Pavilidis, D. *J. Appl. Phys.* **1994**, *76*, 3502.
- Kuwano, N.; Shiraishi, T.; Koga, A.; Oki, K.; Hiramatsu, K.; Amano, H.; Itoh, K.; Akasaki, I. *J. Cryst. Growth* **1991**, *115*, 381.
- Awad, A. K.; Anderson, A. B. *Surface Sci.* **1989**, *218*, 543.
- Wycoff, K. W. G. *Crystal Structures*, 2nd. ed; Wiley: New York, 1964; Vol. 2.
- Chiang, C. -M.; Gates, S. M.; Bensoula, A.; Schultz, J. A. *Chem. Phys. Lett.* **1995**, *246*, 275.
- (a) Anderson, A. B.; Kang, D. B.; Kim, Y. *J. Am. Chem. Soc.* **1987**, *91*, 4245. (b) Mehandru, S. P.; Anderson, A. B. *J. Am. Chem. Soc.* **1985**, *107*, 844. (c) Kang, D. B.; Anderson, A. B. *Surface. Sci.* **1985**, *155*, 639. (e) Kang, D. B.; Anderson, A. B. *Surface. Sci.* **1986**, *165*, 221. (f) Anderson, A. B.; Malony, J. J. *J. Phys. Chem.* **1987**, *92*, 809.

20. Anderson, A. B.; Mehandru, S. P.; Simialek, J. L. *J. Electrochem. Soc.* **1985**, *132*, 1695.
  21. Clementi, E.; Raimondi, D. L. *J. Chem. Phys.* **1963**, *38*, 2686.
  22. Lotz, W. J. *Opt. Soc. Am.* **1970**, *60*, 206.
  23. (a) Mehandru, S. P.; Anderson, A. B.; Brazdil, J. F. *J. Am. Chem. Soc.* **1988**, *110*, 1715. (b) Ward, M. D.; Brazdil, J. F.; Mehandru, S. P.; Anderson, A. B. *J. Phys. Chem.* **1987**, *91*, 6515.
  24. Perry, B.; Rutz, R. F. *Appl. Phys. Letters* **1978**, *33*, 319.
  25. Olson, G. G.; Sexton, J. H.; Lynch, D. W.; Bevolo, A. J.; Shanks, H. R.; Harmon, B. N.; Ching, W. Y.; Wieliczka, D. M. *Solid State Commun.* **1985**, *56*, 35.
  26. Gautier, M.; Durhand, J. P.; LeGressus, C. *Surface Sci.* **1986**, *178*, 201.
  27. Ching, W. Y.; Harmon, B. N. *Phys. Rev.* **1986**, *B34*, 5305.
  28. Hwang, J. S.; Tanaka, S.; Iwai, S.; Aoyagi, Y.; Seong, S. *J. Crystal Growth* **1999**, *200*, 63.
  29. Kim, S. H.; Kim, H. S.; Hwang, J. S.; Choi, J. G.; Chong, P. J. *Chem. Mater.* **1994**, *6*, 278.
  30. Yates, J. T.; Hubner, A. Jr.; Lucas, S. R.; Partlow, W. D.; Schaefer, J.; Choyke, W. J. *Appl. Surf. Sci.* **1994**, *82/83*, 180.
  31. unpublished results.
  32. Wang, K.; Sing, H. J.; Pavlidis, D. *J. Appl. Phys.* **1994**, *76*, 3502.
  33. Almond, M. J.; Drew, M. G. B.; Jenkins, C. E.; Rice, D. A. *J. Chem. Soc., Dalton Trans.* **1992**, 5.
  34. Hwang, J. W.; Campbell, J. P.; Kozubowski, J. K.; Hansen, S. A.; Evans, J. F.; Gladfelter, W. L. *Chem. Mater.* **1995**, *7*, 517.
-